

COMPUTER MODELING OF INTERNAL TARGETS IN ELECTRON STORAGE RINGS\*

R.P. Maloney, R.C. York, J.S. McCarthy, B.E. Norum

Department of Physics  
University of Virginia  
Charlottesville, Virginia 22901

Abstract

The effect of thin ( $1\text{--}50 \mu\text{g}/\text{cm}^2$ ) internal targets on beam quality in electron storage rings is evaluated. The internal target is modeled assuming that scattering is the result of elastic collisions between the beam electrons and the target nuclei. A screened coulomb potential is used and single and plural scattering mechanisms are included. A storage ring particle tracking code, DIMAT,<sup>1</sup> was modified to include the internal target model and used to obtain the results discussed. Beam particle loss distributions and beam envelope "growth times" are given and discussed in light of damping mechanisms inherent in electron storage ring designs.

Introduction

The use of internal targets in electron storage rings may provide a unique method of obtaining high luminosities with very thin targets. Especially in the cases where polarized targets are required, the necessary luminosities may only be achievable through the use of polarized gas jets as targets in storage rings.

The effect on the stored electron beam quality due to the presence of an internal target was analysed for target thicknesses in the range of 1 to  $50 \mu\text{g}/\text{cm}^2$  and electron beam energies in the range of 0.5 to 6 GeV. Computer simulations of the emittance growth due to the beam interaction with the target was done using a storage ring design code to model the magnetic lattice and plural scattering theory to simulate the internal target.

Internal Target Model

The principle effect of the target upon the electron beam is the angular deflection of the beam electrons. The target thicknesses considered were sufficiently small that any translations inside the target would be insignificant, and, were therefore, not included. Energy losses in the target were likewise ignored. The two major contributors to energy loss of the beam electrons in the target are Bremsstrahlung radiation given off as the beam electrons are bent in the nuclear electric field of the target, and collision losses with the atomic electrons in the target. In the regime considered, both of these loss mechanisms were found to be smaller than the average synchrotron energy loss caused by acceleration in the lattice dipole magnets. Since rf power is provided in storage rings to compensate for synchrotron energy losses, there would be no noticeable effect on the beam quality due to energy loss in the internal target, and therefore, energy loss effects were not included in the model of the internal target.

The scattering of beam electrons by the target was simulated using a plural scattering probability distribution. The analysis by E. Kiel et al.<sup>2</sup> and a review article by W.T. Scott<sup>3</sup> were used as the basis of these calculations and the reader is referred to these for a more complete explanation. The relevant equations for scattering are determined by the value of  $\Omega_0$ ; the average number of times a beam electron scatters in a single passage through the target.

$$\Omega_0 \approx \frac{8.847 \times 10^3 \rho t Z^{1/3} (Z+1)}{A B^2}$$

where  $\rho t$  = target thickness ( $\text{gm}/\text{cm}^2$ )

$Z$  = target atomic number

$A$  = target atomic weight.

All targets considered had  $.01 < \Omega_0 < .55$ . In this regime the probability of scattering into  $d\Theta$  about the azimuthal angle  $\Theta$  in the laboratory is:

$$P(\Omega_0, \Theta) d\Theta = \Omega_0 d\Theta \cdot e^{-\Omega_0} (F_1(\psi_{\text{red}}) + \Omega_0^2/2 \cdot F_2(\psi_{\text{red}}))$$

where  $\psi_{\text{red}}$  = the reduced angle =  $\Theta/X_\alpha$

$$\text{and } X_\alpha = \sqrt{1.13 + 3.76 \frac{Z^2 \alpha^2}{B^2}} \cdot \frac{1.13 Z^{1/3}}{137} \left( \frac{\text{mec}}{P} \right)$$

$$F_1(\psi) = \frac{2}{(1+\psi^2)^2}$$

$$F_2(0) = 2/3,$$

$$F_2(\psi) = \frac{4}{\psi^4 (4+\psi^2)^3} \left[ \psi^2 (\psi^4 + 2\psi^2 - 8) + (1+\psi^2) \sqrt{4\psi^2 + \psi^4} \right] \\ * \ln \left[ \frac{(\psi^4 + 4\psi^2 + 2) + (2+\psi^2) \sqrt{4\psi^2 + \psi^4}}{(\psi^4 + 4\psi^2 + 2) - (2+\psi^2) \sqrt{4\psi^2 + \psi^4}} \right]$$

$P(\Omega_0, \psi_{\text{red}})$  is shown as a function of  $\Omega_0$  for different values of  $\psi_{\text{red}}$  in Figure 1 and as a function of  $\psi_{\text{red}}$  for several values of  $\Omega_0$  in Figure 2. For values of  $\Omega_0 > .55$  a more complex procedure was used, and the reader is referred to E. Kiel et al.<sup>2</sup> and W.T. Scott<sup>3</sup> for further discussion.

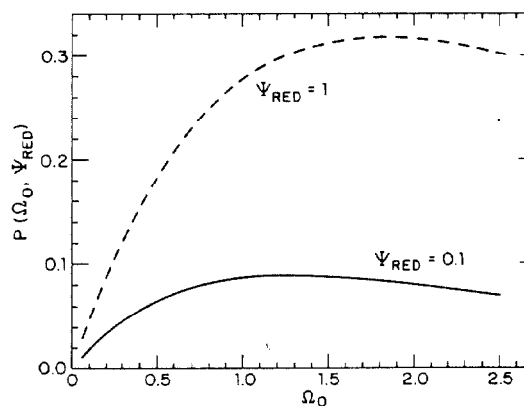


Figure 1.  $P(\Omega_0, \psi_{\text{red}})$  as a function of  $\Omega_0$ .

The probability of scattering through an angle  $\geq \Theta$  is given by

$$G(\Omega_0, \Theta) = \int_{\Theta}^{\infty} d\Theta' P(\Omega_0, \Theta')$$

This is a monotonically decreasing function of  $\Theta$  as shown in Figure 3. The probability distribution  $G(\Omega_0, \Theta)$  was divided into equal probability bins, and the total laboratory scattering angle  $\Theta$  was found through standard Monte Carlo techniques. The scatter-

\* Work supported by the University of Virginia and the Southeastern Universities Research Association (SURA).

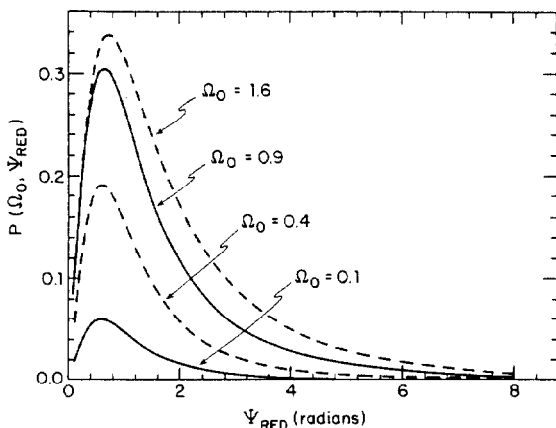


Figure 2.  $P(\Omega_0, \Psi_{\text{RED}})$  as a function of  $\Psi_{\text{RED}}$ .

ing forces are azimuthally symmetric, and therefore, the horizontal and vertical projections of the beam electron deflections were obtained assuming a random distribution.

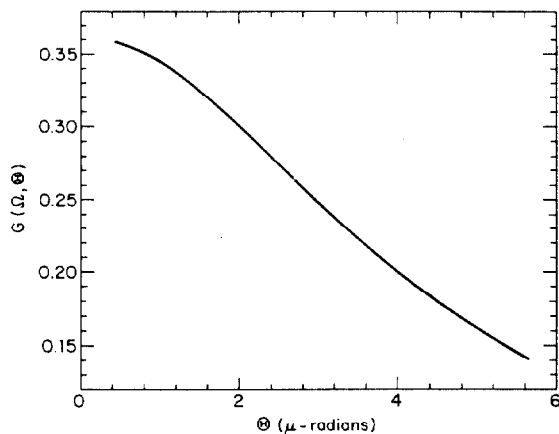


Figure 3.  $G(\Omega, \Theta)$  as a function of  $\Theta$  for the case of  $\Omega_0 = 0.469$  and a beam energy of 2 GeV.

### Simulations

To ascertain the effect on the stored beam emittance due to passage through the internal target, the storage ring design code, DIMAT,<sup>1</sup> was modified to include the internal target model discussed above. To reduce the required computation time to the order of several hours, the storage ring was represented by a single set of first and second order matrices. These matrices were used to track the particles from the exit to the entrance of the target.

Two hundred particles were traced through the storage ring by the modified DIMAT code. The initial phase space distribution was filled assuming a gaussian distribution in energy with  $\sigma = .05\%$ . The transverse phase space was also populated with a gaussian distribution. An emittance of  $0.1 \pi \text{ mm-mr}$  in both planes was used as  $2\sigma$  for this distribution.

The storage ring lattice from which the tracking matrices were obtained consisted of two  $180^\circ$  2I arcs separated by a six cell straight region on either side. The arcs included a dispersion matching region and were based upon the achromat<sup>4</sup> principle. Three families of sextupoles in each plane were used to make chromatic corrections such that no achromatic effects were introduced.<sup>5</sup> One of the straight sections was designed to have beta functions of approximately 7 m in both planes at the target position. This lattice was found

to be linear out to  $20\sigma$  in the transverse phase space where  $1\sigma$  was assumed to be the damped beam emittance.

The results presented in this paper were obtained using the lattice decubed above. However, other lattice designs, such as the SURA pulse stretcher ring<sup>6</sup> were also evaluated with results similar to those given.

The beam emittance as a function of the number of passages through the target was obtained from scatter plots of the particle transverse phase space distributions. The phase space beam ellipse within which approximately 90% of the particles were found were used to determine the emittance. The time for one revolution was assumed to be  $1 \mu\text{s}$ .

### Results

The emittance growth rate due to the presence of an internal target is shown in Figure 4 for the case of  $\Omega_0 = 0.235$  and a beam energy of 2 GeV. The growth time was arbitrarily defined as the time required for the emittance to double from the initial emittance of  $0.1 \pi \text{ mm-mr}$  to  $0.2 \pi \text{ mm-mr}$ . Typical growth times as a function of beam energy and target  $\Omega_0$  are shown in Figures 5 and 6 respectively. The empirical formula,  $\text{time} = \text{constant}/\Omega_0$ , was fit to the growth time as function of  $\Omega_0$ . The curves shown in Figure 6 are the result of this procedure. This function gives a reasonable formulation over the range of  $\Omega_0$  considered.

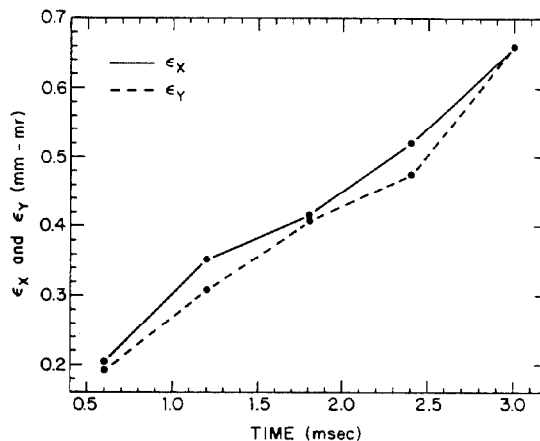


Figure 4. The horizontal and vertical beam emittance growth as a function of time for the case of  $\Omega_0 = 0.235$  and a beam energy of 2 GeV.

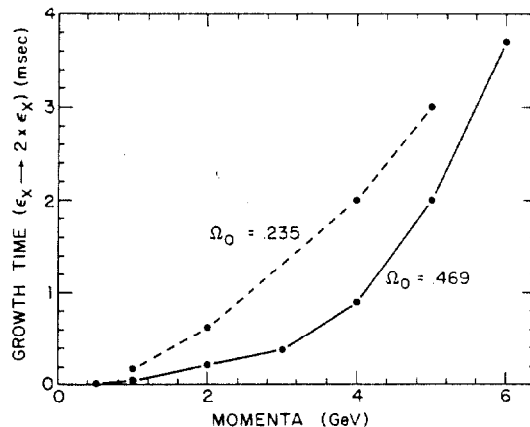


Figure 5. The emittance growth time as a function of energy.

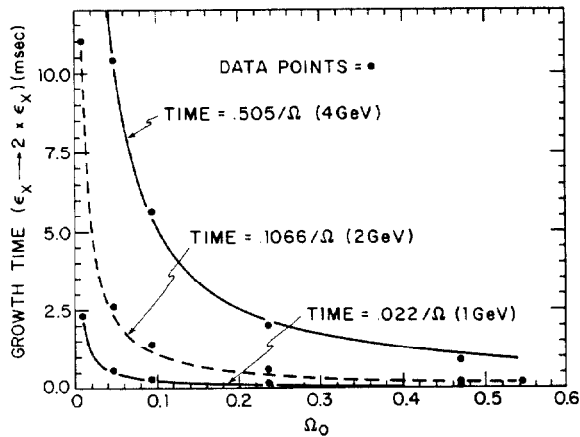


Figure 6. The emittance growth time as a function of  $\Omega_0$ .

#### Conclusions

Emittance growth rates of ones to tens of ms were found for the target thickness and energies evaluated. Since the damping times for storage rings are typically larger than these growth times, they will do little to limit the emittance growth. Therefore, beam store times will be dictated by internal target parameters, the machine admittance, and the beam quality required for the experiments. In any case, parasitic operation of internal targets in electron storage rings does not appear to be an attractive option.

#### References

1. Roger Servranckx, University of Saskatchewan, private communication.
2. E. Keil, *et al.*, "Single and Plural Scattering of Charged Particles", *Zeitschrift für Naturforschung*, Vol. 15 (Dec. 1960) 1031.
3. W.T. Scott, "Theory of Small Angle Multipole Scattering of Fast Charged Particles", *Rev. of Mod. Physics*, Vol. 35 (April 1963) 231.
4. K.L. Brown, "A Second Order Optical Achromat", SLAC-PUB-2257 (Feb. 1979).
5. R.V. Servranckx and K.L. Brown, "Chromatic Corrections for Large Storage Rings", SLAC-PUB-2270 (Feb. 1979).
6. R.C. York, *et al.*, "Multi-GeV Electron Linac-Pulse Stretcher Design Options", these proceedings.